The Products of the Reaction of the Hydroxyl Radical with 2-Ethoxyethyl Acetate

J. R. WELLS* and FLOYD L. WISEMAN

Armstrong Laboratory, Environics Directorate, 139 Barnes Drive, Tyndall Air Force Base, Florida 32403–5323

DALE C. WILLIAMS and J. STEVEN BAXLEY

Applied Research Associates, Gulf Coast Division, P.O. Box 40128, Bldg 1142, Mississippi Road, Tyndall Air Force Base, Florida 32403

D. F. SMITH

ManTech Environmental Technology, Inc., P.O. Box 12313, Research Triangle Park, North Carolina 27709

ABSTRACT

The gas-phase reaction products of the OH radical with 2-ethoxyethyl acetate (EEA, $CH_3C(O)OCH_2CH_2OCH_2CH_3$) have been investigated. 1,2-Ethanediol acetate formate (EAF, $CH_3C(O)OCH_2CH_2OC(O)H$) and ethyl formate (EF, $HC(O)OCH_2CH_3$) were identified as the two main products. A third product, ethylene glycol diacetate (EGD, $CH_3C(O)OCH_2CH_2OC(O)CH_3$), was also observed. EAF, EF, and EGD formation yields were determined to be 0.37 ± 0.03 and 0.328 ± 0.018 and 0.040 ± 0.005, respectively. Proposed reaction mechanisms are discussed and compared with these data. © 1996 John Wiley & Sons, Inc.

INTRODUCTION

The US Air Force in the course of its normal, peacetime operations performs many regular activities which result in the emission of volatile organic compounds (VOC). A common maintenance operation is the stripping and repainting of aircraft. This process requires large quantities of organic solvents that evaporate into the atmosphere. The Department of Defense (DoD) has committed itself to complying with local and state regulation. Therefore, the impact of these evaporated solvents must be evaluated. In addition, there is a need for understanding the fundamental effects a VOC has on local and global regions. These effects can be considered by the following series of questions: (1) What is the atmospheric lifetime of the emitted VOC; (2) What are the identities and yields of the products formed during the atmospheric degradation of the VOC; and (3) Is the VOC effective in producing tropospheric ozone when oxidized in the presence of NO_x? The answers to these questions are ultimately grounded in understanding the gas-phase kinetics and mechanisms of these compounds when photooxidized under atmospheric conditions.

As part of ongoing Air Force research to charac-

Received September 12, 1995; accepted January 2, 1996

* Author to whom correspondence should be addressed.

International Journal of Chemical Kinetics, Vol. 28, 475–480 (1996)

© 1996 John Wiley & Sons, Inc. CCC 0538-8066/96/070475-06

terize the atmospheric transformations of VOC and address their potential environmental impact, we report the product identification and yield data for the reaction of OH with 2-ethoxyethyl acetate (EEA), a paint component and solvent currently used by the Air Force in sizable quantities.

EXPERIMENTAL

Apparatus and Materials

Experiments to measure the yields of the reaction products of OH with EEA were conducted with a previously described apparatus [1,2]. A brief description is provided here for convenience. Reactants were introduced and samples were withdrawn through a 6.4-mm Swagelok fitting attached to ca. 100 L Teflon™ film chamber. Dry compressed air was added as a diluent to the reaction chambers and measured with a 0–100 L-min^{-1} mass flow controller. The filler system was equipped with a syringe injection port facilitating the injection of both liquid and gaseous reactants into the chambers in a flowing airstream. All reactant mixtures and calibration standards were generated by this system. Irradiations of the Teflon™ chamber contents were performed in an enclosure containing six 40-watt black lamps (GE F40 BLB) and four 40-watt sun lamps (Westinghouse F40). A fan cooled the inside of the enclosure, maintaining a reaction temperature of approximately 25°C.

Reactant and product concentrations were measured by gas chromatography (GC) and high pressure liquid chromatography (HPLC). Gas samples for GC analysis were cryogenically collected on a Hastelloy C sample loop (ca. 1.3 mL) and injected onto the GC column with a heated rotary valve [3]. Samples were drawn through the inlet system by a pump and a 0–100 mL min^{-1} mass flow controller. Typically, 100 mL samples were collected in the sample loop cooled to − 100°C, flash heated, and focused onto the gas chromatograph column.

Analyses of the organic components before and after the timed irradiations were performed using an Hewlett-Packard (HP) 5890A GC equipped with a flame ionization detector (FID). Data were collected, stored, and analyzed on a computer using HP 3365 Series II Chemstation software. The compounds were separated by a Restek Rtx®-20 column (0.53-mm i.d., 30-m length, 1.0-μm film thickness) connected to the heated rotary valve using a press tight connector. Helium was used as the carrier gas.

Product identifications experiments were performed in a 3000 L Teflon™ chamber. The reactants were irradiated with 34 black lamps (GE F40 BLB) and 14 sun lamps (GE F40 CW). The chamber mixture was sampled by cryogenic collection method identical to the product yield experiments described above except with a sample volume that was twice as large and analyzed with an HP 5890 Series II Plus GC/HP 5971 mass selective detector/HP 5965B infrared detector (GC/MS/FTIR) system. Compound separation was achieved by a Supelco SPB®-20 column (0.32-mm i.d., 30-m length, 0.25-μm film thickness). The chamber contents were also analyzed by long path infrared spectroscopy. The infrared beam of a Nicolet 740 Fourier Transform Infrared (FTIR) spectrometer traversed the chamber using conventional White cell optics [4]. An absorption path length of approximately 70 m was used to monitor the *entire* chamber contents during the course of the reaction.

Carbonyl compounds produced by gas-phase reactions were measured by impinger sampling in a derivatizing solution of 2,4-dinitrophenylhydrazine (DNPH). Hydrazones formed by derivatization were separated and quantitatively measured by HPLC (HP 1050) using a three component gradient solvent program as described previously [5].

OH, the primary oxidizing radical in the troposphere, was generated from the photolysis of methyl nitrite (CH_3ONO) in the presence of nitric oxide (NO) in air [6]. CH_3ONO was prepared in gram quantities using the method of Taylor *et al.* [7] and stored in a lecture bottle at room temperature. The CH_3ONO purity was verified by GC/MS/FTIR.

Ethylene glycol diacetate, 2-ethoxyethyl acetate, and ethyl formate were obtained from Aldrich Chemical Company and used as supplied. Ethanediol acetate formate was synthesized by Radian Corporation and used as supplied. Nitric oxide (NO) was obtained from Matheson Gases and used as supplied. Helium, UHP grade, used in the product identification experiments was purchased from Air Products and passed through a drying trap before use. Helium for the quantitation experiments was supplied by Tyndall Air Force Base and passed through drying and hydrocarbon removal cartridges before use.

Experimental Procedures

Identification of products formed during the irradiation were obtained by GC/MS/FTIR. The concentrations of the pertinent species in the 3000 L chamber were 12–18 ppm EEA, 10–25 ppm CH_3ONO, and 5–7 ppm NO in air. For MS/FTIR measurements this mixture was irradiated for timed (one, two, or four min) intervals followed by sample collection. The mass selective detector was tuned before each experimental run using perfluorotributylamine (FC-43). Full scan electron impact ionization spectra were collected from 25 to 220 mass units. The infrared detector (GC/MS/FTIR) was operated at eight cm^{-1} resolution with each four scans averaged to give a single IR spectrum every 1.5 s. The long path FTIR was operated at one cm^{-1} resolution and an infrared spectrum of the entire chamber contents was collected after *each* irradiation. Preliminary compound identifications from the GC/MS/FTIR data sets were made by searching the Wiley/NBS Mass Spectra Library and the EPA vapor library. Pure samples of the identified products were obtained to check for matching spectra (MS and FTIR) and retention time.

Product samples for quantitative analysis were collected on the cryogenic sample loop for four min at 25 mL min^{-1} and then flash injected onto the column. The concentrations of the pertinent species in the small chamber were 5–9 ppm EEA, 5–10 ppm CH_3ONO, and 2–5 ppm NO in air. The FID signal was used to determine reactant and product concentrations and calibrated with known concentrations of the identified products and reactant. Pure samples of the identified products were obtained to check for matching retention time and calibration.

RESULTS

The OH rate constant for EEA was measured previously [2,8]. A rate constant of $10.56 \pm 1.31 \times 10^{-12}$ $cm^3 molec^{-1} s^{-1}$ was observed in ref. [2], yielding an atmospheric ($1/e$) lifetime of 26 h using $[OH] = 1 \times 10^6$ molecules cm^{-3}. In these experiments, the OH radical generated from the photolysis of methyl nitrite is the primary oxidizing species [2]. The three major products of the reaction between OH and EEA found from the GC/MS/FTIR experiments are 1,2-ethanediol acetate formate (EAF), ethylene glycol diacetate (EGD), and ethyl formate (EF).

The GC/FID apparatus was used for quantitative data collection as described in the Experimental section. A plot of the OH + product corrected concentrations of the three main products EAF, EGD, and EF vs. the concentration of EEA lost due to reaction with OH is displayed as Figure 1. The EAF is *displaced* on the y axis by + 0.3 ppm units to avoid confusion with the EF data points. The data points at the origin are experimental points because preirradiation, $t = 0$, data showed no traces of any of the products. The amount of EEA reacted is determined as the difference between the initial concentration and the concentration after an irradiation ($[EEA]_0 - [EEA]_t$). These plots are the cumulative results of five separate experiments of three or four irradiations each. The product yields were computed from the slope of an unrestricted linear least-squares fit to the data. The data, corrected for OH/product reactions, is plotted in Figure 1 and gives yields for EAF, EGD, and EF of 0.37 ± 0.03, 0.040 ± 0.005, and 0.33 ± 0.02, respectively. The error limits given are the 95% confidence intervals for the slopes of the linear least-squares analyses.

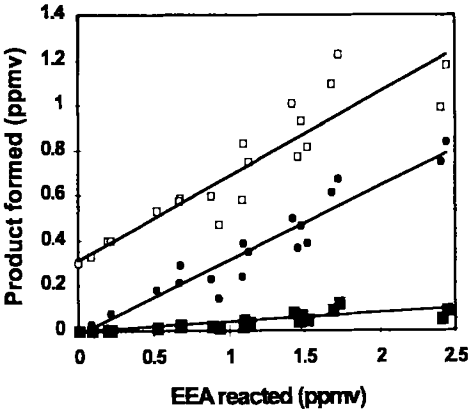

Figure 1 Plot of products EAF (□), EGD (■), and EF (●) formed vs. 2 ethoxyethyl acetate (EEA) reacted. Ethanediol acetate formate (EAF, $CH_3C(O)OCH_2CH_2OC(O)H$) is shifted up on the y axis by +0.3 ppmv units to avoid confusion with ethyl formate (EF, $HC(O)OCH_2CH_3$). The slopes of the linear least-squares analysis with 95% confidence intervals are 0.37 ± 0.03, 0.040 ± 0.005, and 0.33 ± 0.02 for EAF, EGD, and EF, respectively.

The other products observed were at very low concentrations and would thus have little impact on the development of a reaction mechanism, but will be noted here for completeness. Ethylene glycol monoacetate ($CH_3C(O)OCH_2CH_2OH$), acetic acid ($CH_3C(O)OH$), acetaldehyde (CH_3CHO), and an unusual product proposed to be ethyl 2-(acetyloxy)acetate, $CH_3C(O)OCH_2C(O)OCH_2CH_3$, were all consistently observed products from the large chamber experiments. Both formaldehyde (H_2CO) and acetaldehyde (CH_3CHO) were observed in DNPH derivatization experiments. Formaldehyde is a product of methyl nitrite photolysis. The unusual product's hypothesized structure, $CH_3C(O)OCH_2C(O)OCH_2CH_3$, was determined from mass spectral data only. Carbon monoxide (CO) concentration, observed by long path FTIR, was greater than was observed from photolysis of methyl nitrite/NO/air. This suggests that the CO concentration observed was due to methyl nitrite/NO photolysis reactions *and* as a product of the reaction of OH with EEA.

The method adopted to evaluate the effect of secondary reactions on the observed yields of products uses a two step mechanism, the formation of a product (P) due to reaction of OH + EEA followed by OH + P. This approach, which has been previously described in detail [9,10], yields an expression of the following form:

$$F = \frac{(k_R - k_P)}{k_R} \times \frac{1 - \dfrac{[\mathrm{EEA}]_t}{[\mathrm{EEA}]_0}}{\left(\dfrac{[\mathrm{EEA}]_t}{[\mathrm{EEA}]_0}\right)^{k_P/k_R} - \dfrac{[\mathrm{EEA}]_t}{[\mathrm{EEA}]_0}}$$

F represents the correction, k_R the rate constant for the reaction of OH with EEA, and k_P the rate constant for the reaction of OH with P. This expression was applied to the EAF, EF, and EGD data. The rate constant for OH + EF ($1.02 \pm 0.14 \times 10^{-12}$ cm^3 molecule^{-1} s^{-1}) measured by Wallington, et al. [11] was used, while the OH rate constants for EAF and EGD were calculated using the method of Kwok and Atkinson [12] (3.8×10^{-12} cm^3 molecule^{-1} s^{-1} for EAF and 3.9×10^{-12} cm^3 molecule^{-1} s^{-1} for EGD). The average correction, F, for EAF, EGD, and EF was 4.5%, 4.7%, and 1.2%, respectively.

DISCUSSION

OH reacts with EEA by H-atom abstraction. A reaction mechanism, based upon the observed products is proposed in Figure 2. EEA is a large molecule with *five* possible carbon–hydrogen sites for OH radical attack. However, the products of the reaction of OH with EEA suggest strongly that the OH abstracts hydrogen principally from either of the two methylene groups bonded to the ether oxygen of the ethoxy functional group;

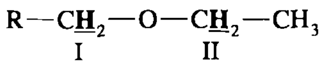

$$\mathrm{R{-}\underset{I}{C\underline{H}_2}{-}O{-}\underset{II}{C\underline{H}_2}{-}CH_3}$$

Structure 1

where the R-group is $\mathrm{CH_3{-}C(O){-}O{-}CH_2{-}}$. This is consistent with the few literature reports which suggest that the OH radical reacts predominantly with the alkoxy end of an ester rather than the acyl end [11,13–15].

The experimental parameters were set to minimize other side reactions and highlight the first OH hydrogen abstraction step. Nitric oxide (NO) was added to facilitate the generation of OH and to minimize ozone (O_3) and NO_3 formation and thus prevent other possible radical reactions. The OH generation was controlled by minimizing the total photolysis time so that only 20–30% of the EEA was removed by the primary reaction. This decreased the possibility of the OH + EEA reaction products reacting with the OH and generating *another set of products.* A mechanism which explains the products observed is as follows with the substantial branches depicted in Figure 2. Both the products EAF and EGD are structurally similar to EEA (Fig. 2) and certainly result from the same initial hydrogen abstraction step at the right methylene (II) group in Structure 1. Depending on the nature of the alkoxy radical formed in Reaction (2);

$$\text{R-CH}_2\text{-O-CH}_2\text{-CH}_3 + \text{OH}\bullet \longrightarrow \text{R-CH}_2\text{-O-(CH}\bullet\text{)-CH}_3 + \text{H}_2\text{O} \tag{1}$$

$$\text{R-CH}_2\text{-O-(CH}\bullet\text{)-CH}_3 + \text{O}_2 + \text{NO} \longrightarrow \text{R-CH}_2\text{-O-(CHO}\bullet\text{)-CH}_3 + \text{NO}_2 \tag{2}$$

$$\text{R-CH}_2\text{-O-(CHO}\bullet\text{)-CH}_3 + \text{O}_2 \longrightarrow \text{R-CH}_2\text{-O-C(O)-CH}_3\ \textbf{(EGD)} + \text{HO}_2 \tag{3}$$

$$\text{R-CH}_2\text{-O-(CHO}\bullet\text{)-CH}_3 \longrightarrow \text{R-CH}_2\text{-O-CHO}\ \textbf{(EAF)} + \bullet\text{CH}_3 \tag{4a}$$

$$\text{R-CH}_2\text{-O-(CHO}\bullet\text{)-CH}_3 \longrightarrow \text{R-CH}_2\text{-O}\bullet + \text{CH}_3\text{-CHO (acetaldehyde)} \tag{4b}$$

$$\text{R-CH}_2\text{-O-CH}_2\text{-CH}_3 + \text{OH}\bullet \longrightarrow \text{R-(CH}\bullet\text{)-O-CH}_2\text{-CH}_3 + \text{H}_2\text{O} \tag{5}$$

$$\text{R-(CH}\bullet\text{)-O-CH}_2\text{-CH}_3 + \text{O}_2 + \text{NO} \longrightarrow \text{R-(CHO}\bullet\text{)-O-CH}_2\text{-CH}_3 + \text{NO}_2 \tag{6}$$

$$\text{R-(CHO}\bullet\text{)-O-CH}_2\text{-CH}_3 \longrightarrow \text{CH}_3\text{-CH}_2\text{-O-C(O)H}\ \textbf{(EF)} + \text{R}\bullet \tag{7a}$$

$$\text{R-(CHO}\bullet\text{)-O-CH}_2\text{-CH}_3 \longrightarrow \text{R-CHO} + \bullet\text{O-CH}_2\text{-CH}_3 \tag{7b}$$

$$\text{R-(CHO}\bullet\text{)-O-CH}_2\text{-CH}_3 + \text{O}_2 \longrightarrow \text{R-C(O)-O-CH}_2\text{-CH}_3 + \text{HO}_2 \tag{8}$$

$$\text{CH}_3\text{-C(O)-O-CH}_2\bullet + \text{O}_2 + \text{NO} \longrightarrow \text{CH}_3\text{-C(O)-O-CH}_2\text{O}\bullet + \text{NO}_2 \tag{9}$$

$$\text{CH}_3\text{-C(O)-O-CH}_2\text{O}\bullet + \text{O}_2 \longrightarrow \text{CH}_3\text{-C(O)-O-CHO}\bullet + \text{HO}_2 \tag{10}$$

it can form EGD (Reaction (3)) through further reaction with O_2 or it can decompose through one of two pathways to form EAF (Reaction (4a)) or acetaldehyde ($\mathrm{CH_3{-}CHO}$) (Reaction (4b)) plus another alkoxy radical, $\mathrm{R\text{-}CH_2{-}O\bullet}$. Further decomposition of $\mathrm{R\text{-}CH_2{-}O\bullet}$ radical could follow a similar reac-

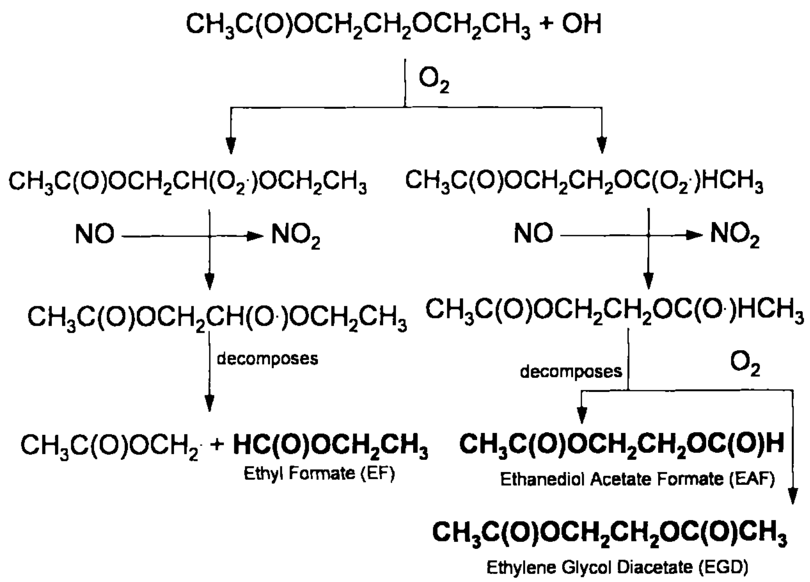

Figure 2 Proposed reaction mechanism for hydroxyl radical with 2 ethoxyethyl acetate. Major products are in bold typeface.

tion sequence as shown in Reactions (9) and (10) eventually resulting in the same products as for the R• radical from Reaction (7a).

The other major product observed is ethyl formate, EF; CH_3-CH_2-O-C(O)H, formed from hydrogen abstraction from the inner or left methylene group, I in Structure 1, depending on the disposition of the alkoxy radical formed in Reaction (6) above. If the radical decomposes according to Reaction (7a), the result is ethyl formate, but if it decomposes by Reaction (7b), the result is an unobserved product, R-CHO, plus an alkoxy radical, which likely oxidizes to form acetaldehyde. The product of Reaction (8), R-C(O)-O-CH_2-CH_3, was identified as a consistently observed peak on the mass spectrum total ion chromatogram after OH reaction with EEA. The mass spectrum of this compound was not matched in the mass spectral library, but a structure of $CH_3C(O)OCH_2C(O)OCH_2CH_3$ is a reasonable match of the observed mass spectrum. If this is the diester product formed in Reaction (8) it is assumed that primary pathway was through decomposition as in Reactions (7a) and (7b).

If disposition of the R• radical formed in Reaction (7a) followed Reactions 9 and 10 formic acetic anhydride (Reaction (10)) would result. In the presence of any water, this would decompose to acetic acid ($CH_3C(O)OH$) and formic acid, both of which were consistently observed in the GC/MS/FTIR and GC experiments. The alkoxy radical formed in Reaction (9) could also decompose possibly resulting in the products carbon monoxide, carbon dioxide, formaldehyde, and acetyl radicals. Carbon monoxide was observed in the large chamber reaction system by long path FTIR. Under urban conditions, the acetyl radicals could subsequently result in the formation of peroxyacetyl nitrate (PAN) [16,17].

The ratio of EAF to EGD formed in the reaction is about 10:1, indicating the primary pathway for disposition of the alkoxy radical formed in Reaction (5) is through decomposition. Ethyl formate is also formed through decomposition of the alkoxy radical form Reaction (6). Further, the formation of acetaldehyde from other decomposition pathways indicated the primary fate of the alkoxy radical adjacent to the ether linkage is through decomposition. This is in agreement with a previously published report on reaction of OH with the branched ether, ethyl *t*-butyl ether [18]. In this case, the primary point of attack by OH is on the methylene group of the ethyl side of the ether, similar to EEA.

The linear relationship between products formed vs. EEA lost shown in Figure 1 indicates that EAF, EGD, and EF are not lost or produced by any other side reactions. This supports the proposed OH/EEA reaction mechanism in Figure 2. The structure of the measured products EGD, EAF, and EF are such that they could not have come from the same EEA molecule resulting in the observation of products from almost 74% of the total EEA reacted. However, the *total* carbon recovered was about 51% with the primary error occurring from the balance of products not observed following the formation of ethyl formate.

Using the method outlined in ref. [12], calculation of the OH + EEA rate constant supports the observations and reaction mechanism (Fig. 2) presented in this article. Sites I and II on Structure 1 make the largest contribution to the calculated OH rate constant, indicating that these are the most reactive sites on EEA for hydrogen abstraction by OH.

CONCLUSION

The OH radical abstracts hydrogen principally from either of the two methylene groups bonded to the ether oxygen of the ethoxy functional group of EEA. The major radical formed from the reaction of OH with EEA, CH_3-C(O)-O-CH_2-CH_2-O-(CHO•)-CH_3 can proceed to produce EGD in low yield or decompose to produce EAF in higher yield. The other principal product, EF, is formed by decomposition of the CH_3-C(O)-O-CH_2-(CHO•)-O-CH_2-CH_3 radical. The observed yields for EAF, EGD, and EF are 0.35 ± 0.02, 0.0369 ± 0.005, and 0.32 ± 0.02, respectively. Other products observed in lower yields and not quantified include formic acid, carbon monoxide, acetic acid, acetaldehyde (CH_3CHO), and ethylene glycol monoacetate ($CH_3C(O)OCH_2CHOH$). An unusual compound identified by mass spectrum is most likely ethyl 2-(acetyloxy)acetate, $CH_3C(O)OCH_2C(O)OCH_2CH_3$.

BIBLIOGRAPHY

1. L. N. O'rji and D. A. Stone, *Int. J. Chem Kinet.*, **24,** 703 (1992).
2. D. C. Williams, L. N. O'rji, and D. A. Stone, *Int. J. Chem. Kinet.*, **25,** 539 (1993).
3. D. F. Smith, T. E. Kleindienst, E. E. Hudgens, and J. J. Bufalini, *Intern J. Environ. Anal. Chem.*, **54,** 265 (1994).
4. J. U. White, *J. Opt. Soc. Am.*, **32,** 285 (1942).
5. D. F. Smith, T. E. Kleindienst, and E. E. Hudgens, *J. Chromatog.*, **483,** 431 (1989).
6. R. Atkinson, W. P. L. Carter, A. M. Winer, and J. N. Pitts, Jr., *J. Air Pol. Control*, **31,** 1090 (1981).
7. W. D. Taylor, D. Allston, M. J. Moscato, G. D. Fazekas, R. Kozlowski, and G. A. Takacs, *Int. J. Chem. Kinet.*, **12,** 231 (1980).
8. D. Hartman, A. Gedra, D. Rhasa, and R. Zellner, *Proceedings of the 4th European Symposium of Physico-Chemical Behavior of Atmospheric Pollutants*, Riedel, Dordecht, The Netherlands, 1987.
9. D. F. Smith, C. D. McIver, and T. E. Kleindienst, *Int. J. Chem. Kinet.*, **27,** 453 (1995).
10. R. Atkinson, S. M. Aschmann, W. P. L. Carter, A. M. Winer, and J. N. Pitts, Jr., *J. Phys. Chem.*, **86,** 4563 (1982).
11. T. J. Wallington, P. Dagaut, R. Liu, and M. J. Kurylo, *Int. J. Chem. Kinet.*, **20,** 177 (1988).
12. E. S. C. Kwok and R. Atkinson, *Atmos. Environ.*, **29,** 1685 (1995).
13. I. M. Campbell and P. E. Parkinson, *Chem. Phys. Lett.*, **53,** 385 (1978).
14. A. M. Winer, A. C. Lloud, K. R. Darnall, R. Atkinson, and J. N. Pitts, Jr., *Chem. Phys. Lett.*, **51,** 221 (1977).
15. J. A. Kerr and D. W. Stocker, *J. Atmos. Chem.*, **4,** 253 (1986).
16. J. H. Seinfeld, *Atmospheric Chemistry and Physics of Air Pollution*, Wiley, New York, 1986.
17. B. J. Findlayson-Pitts and J. N. Pitts, Jr., *Atmospheric Chemistry: Fundamentals and Experimental Techniques*, Wiley, New York, 1986.
18. D. F. Smith, T. E. Kleindienst, E. E. Hudgens, C. D. McIver, and J. J. Bufalini, *Int. J. Chem. Kinet.*, **24,** 199 (1992).